International Journal of Power Electronics and Drive System (IJPEDS)
Vol. 17, No. 3, September 2026, pp. 1982~1993
ISSN: 2088-8694, DOI: 10.11591/ijpeds.v17.i3.pp1982-1993

THD reduction in a 13-level multilevel inverter using the angle control technique

Dewan Ashikur Rahaman, Aive Alamgir, Md Ashraf Hossain, Tapan Kumar Chakraborty, Raisul Islam Rafi, Raiyan Rahman Zihad, Md. Abdullah Al Mahmud, Samia Sarkar
Department of Electrical and Electronic Engineering, University of Asia Pacific, Dhaka, Bangladesh

Article Info

Article history:

Received Mar 5, 2026
Revised Jul 21, 2026
Accepted Aug 14, 2026

Keywords:

Angle
Equal step angle
Inverter
Multilevel inverter
Total harmonic distortion

ABSTRACT

When compared to a traditional multilevel inverter, multilevel inverters can produce switched waveforms with lower amounts of harmonic distortion. Due to their capacity to provide excellent output waveforms at lower switching frequencies and without distortion, multilevel inverters have recently attracted more attention. The dynamic voltage restorer's multilevel topology reduces the output waveform's harmonic distortion without causing inverter power output losses. This study examines the most widely used topologies to determine how the sinusoidal switching angle affects total harmonic distortion (THD%). Among the crucial multilevel topologies, the cascaded H-bridge was selected. Because it needed fewer parts than the others. Asymmetric was selected for observation and simulations of output voltages up to Fifteen levels for equal and sinusoidal angles using PSIM software after a review of the literature. Appropriate switching angles were maintained in this research. With fewer H-bridges, higher-level multilevel inverters have been manufactured.

Corresponding Author:

Dewan Ashikur Rahaman
Department of Electrical and Electronic Engineering, University of Asia Pacific
74/A, Green Road, Dhaka 1205, Bangladesh
Email: ashik@uap-bd.edu

1. INTRODUCTION

A multilevel inverter (MLI) is a type of power electronics system that converts multiple low-level DC inputs into an AC output with adjustable frequency and voltage [1]. Multilevel inverters (MLIs) are sophisticated iterations of two-level inverters designed for medium- and high-power applications [2]. The three-level converter [3] served as the foundational concept that initiated the evolution of MLIs. They consist of a network of power semiconductors and capacitive voltage sources that can deliver a stepped voltage waveform resembling a sinusoidal shape when interconnected and regulated [4]. The growing use of renewable energy sources, including solar photovoltaic and wind energy systems, necessitates the development of cutting-edge technology for efficient integration [5]. Multilevel inverters (MLIs) offer superior output waveform quality, reduced harmonic distortion, improved electromagnetic compatibility, and a modular structure, making them suitable for a wide range of applications [6]. Their efficiency, high voltage capacity, and improved performance make these devices highly attractive in power electronics [7], [8].

Conventional multilevel inverter topologies like flying capacitor, diode-clamped, and cascaded H-bridge converters face a rapid increase in power devices with higher output voltage levels. This exponential growth complicates the inverter, resulting in increased costs, losses, and more stringent control and thermal management needs [8]. Various topologies were proposed to address the issues with conventional MLI [9], [10]. Prior studies [11] have highlighted the limitations associated with conventional modular structures. Alishah *et al.* [12] introduced a topology with two reverse-connected T-type structures, achieving a 9-level output without an H-bridge. Hosseinzadeh *et al.* [13] proposed a modified H-bridge inverter using diodes, capacitors, and multiple DC sources to create various voltage levels, with capacitors charged to twice the input voltage for enhanced modulation performance.

Multilevel inverters (MLIs) use multiple inverter units to generate specified AC voltage levels from various DC sources [14]-[16]. While their stepped output can introduce harmonic challenges, producing voltage in smaller increments ultimately improves power quality. These advantages have driven growing research interest in MLIs. MLIs exhibit several limitations, most notably the requirement for numerous power switches, which increases design complexity [17]-[20]. Although low-voltage switches can be used, each device still needs dedicated gate-driving and protection circuitry, thereby elevating cost and system intricacy. To mitigate these challenges, various innovative MLI configurations have been proposed that reduce the number of DC sources and bridge switches relative to conventional architectures [21], [22]. However, in order to generate output voltages with consistent step levels, many of these more recent inverters still rely on numerous bidirectional switches [23], [24].

Research on cascaded multilevel inverters (MLIs) has shown that various configurations, such as unidirectional switches, enable higher output voltage levels while reducing component counts and costs [23]. However, challenges persist regarding the need for larger DC-link voltages and effective multilayer modulation techniques. Most existing studies have focused on equal-step switching-angle methods, lacking a systematic comparison with sinusoidal switching-angle techniques under identical operating conditions [25]. Switching angles determine the inverter switching instants and directly control the harmonic content of the output voltage [26]. One switching angle is used to regulate the fundamental voltage, while the remaining angles are selected to eliminate specific low-order harmonics [27]. Thus, with (m) switching angles, up to (m-1) harmonic orders can be eliminated by solving the corresponding harmonic equations. This study addresses the limitations of previous MATLAB-based methods for identifying switching angles in modulation performance by employing PSIM due to its user-friendly simulation capabilities. It compares equal-step and sinusoidal switching-angle methods for a 13-level cascaded H-bridge inverter, utilizing a consistent analytical approach supported by both simulations and laboratory experiments. The results indicate that both methods achieve very low total harmonic distortion (THD), providing valuable insights for implementation.

2. METHOD

Determining conduction (switching) angles in an MLI is critical for generating proper gating signals. Two methods are commonly used: the equal-angle technique, which applies uniform conduction periods, and the sinusoidal-angle technique, which varies these periods based on a defined formula. The formula is shown in (1).

$$\theta = \sin^{-1}\left(\frac{Vo}{Vm}\right) \tag{1}$$

Where Vo denotes the output voltage at a specific moment, while Vm denotes the peak voltage of that level. For example, to develop a 5-level multilevel inverter using (1).

To develop a 5-level MLI is required: number of H-bridges = 2, number of IGBTs = 8, number of DC sources = 2, and number of gate pulses = 8. We know that for a complete cycle time period, T = 360° and for a 50 Hz signal, T = $\frac{1}{F}$ = $\frac{1}{50}$ = 0.02 sec. In Figure 1, the expected output of 5-level MLI is shown. The calculation process for each angle is like:

- When the supply voltage V1 = 0v, $\theta = \sin^{-1}\frac{0\,V}{24\,V}$ = 0 °
- When the supply voltage V2 = 12v, $\theta = \sin^{-1}\frac{12\,V}{24\,V}$ = 30 °
- When the supply voltage V3 = 24v, $\theta = \sin^{-1}\frac{24\,V}{24\,V}$ = 90 °
- When the supply voltage V1 = -12v, $\theta = \sin^{-1}\frac{-12\,V}{24\,V}$ = -30 °
- When the supply voltage V1 = -24v, $\theta = \sin^{-1}\frac{-24\,V}{24\,V}$ = -90 °

The workflow presented in Figure 2 follows several essential stages. Initially, a switching device like an IGBT or MOSFET is chosen. The inverter level is defined, and the circuit is modeled in PSIM with predetermined switching angles for Equal Step and Sinusoidal Angle approaches. The simulation generates output waveforms, which are analyzed for FFT spectrum and THD values, organized in tabular form. The methodology of this work is shown in Figure 2.

The proposed MLI circuit, depicted in Figure 3, features three H-bridge inverter modules connected in series, with each module supplied by a separate DC source (12 V, 24 V, and 36 V) from batteries to achieve a specific output voltage. This design eliminates the need for capacitors or voltage-clamping diodes due to the series connection of AC terminal voltages within the cascaded inverter structure. Each inverter unit utilizes one of four IGBT switches (IGBT-1, IGBT-2, IGBT 3, and IGBT-4), uniquely identified for each level inverter. The multilayer output is achieved through a driver circuit that activates IGBTs in a primary multilevel inverter [26]. This setup uses four IGBTs to create a single-phase cascaded asymmetrical switching DC voltage source MLI, resulting in three levels of DC voltage. The load receives a 13-level AC output voltage from an H-bridge with an additional sixteen IGBTs.

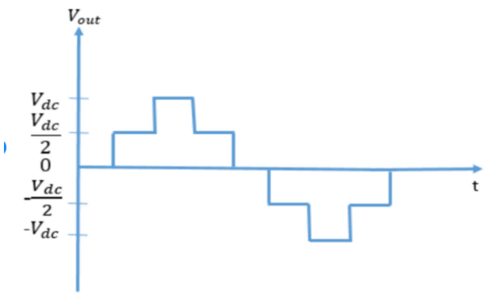

Figure 1. Expected output waveform of 5-level MLI

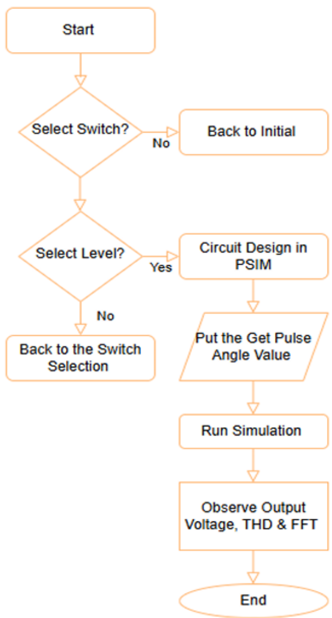

Figure 2. Workflow diagram

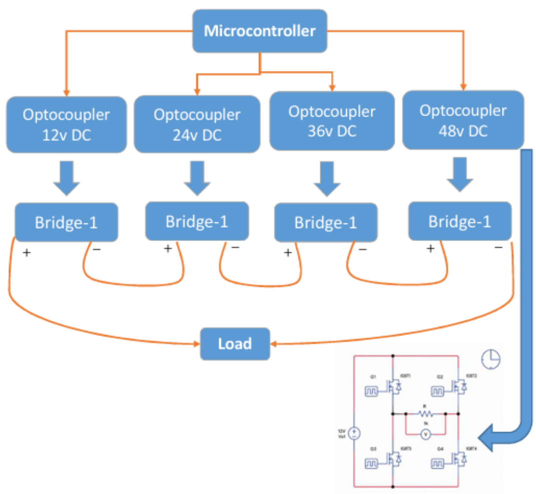

Figure 3. Experimental workflow of this research

3. RESULTS AND DISCUSSION

Numerous software platforms-such as PSPICE, Proteus PSIM, MATLAB/Simulink, and Multisim-are available for electronic circuit simulation. Among them, PSIM is widely regarded as especially effective for modeling and analyzing power electronic systems [3]:

i) Very fast simulation speed, especially for high-frequency switching circuits;
ii) User-friendly interface with easy schematic design and minimal setup time;
iii) Stable and accurate modeling of switching devices (MOSFETs, IGBTs, Diodes);
iv) Supports MATLAB/Simulink co-simulation for advanced control designs; and
v) Provides built-in tools for FFT, THD, and performance analysis.

The schematic diagrams of the 13-level MLI are shown in Figure 4. In this design, 12 IGBTs are used to form three H-bridges, and the load terminal is connected to a resistive load. The output voltage is measured across this load. Three asymmetrical DC voltage sources (12 V, 24 V, and 36 V) are used at the supply terminal. Gating pulses are applied to the IGBT gate terminals to control their switching states and the operation of each H-bridge. The switching angles for the gate pulses were calculated manually for both cases.

The proposed angle control method effectively eliminates certain lower-order harmonics while maintaining the fundamental voltage, thereby setting the switching angles. This approach significantly reduces switching losses, voltage stress on power devices, and total harmonic distortion (THD). The system's harmonic performance is evaluated by examining the voltage waveform delivered to a 1 kΩ resistive load.

The output of this work has been generated in PSIM software. For the 13-level inverter, the output voltage has been measured across the load resistor. For both of the methods, equal-step switching angle and sinusoidal switching angle, the output voltage has been shown in Figure 5 and Figure 6. The angles are determined through manual calculation for equal-step switching, and for sinusoidal angle switching, the proposed formula has been used, which is mentioned in (1). The voltage output waveforms are shown in Figure 5, where VP1 on the y-axis denotes the value of the output voltage and the x-axis denotes time in milliseconds.

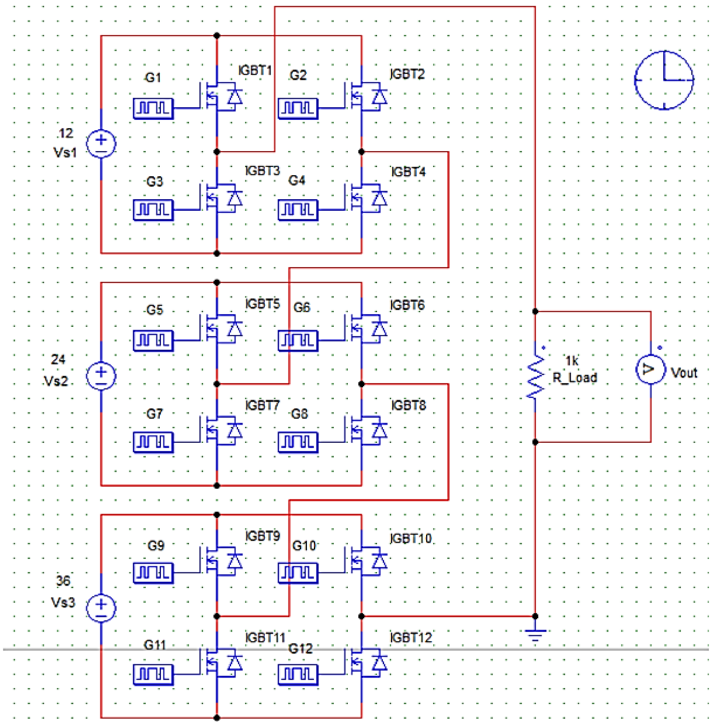

Figure 4. Circuit diagram of 13-level MLI

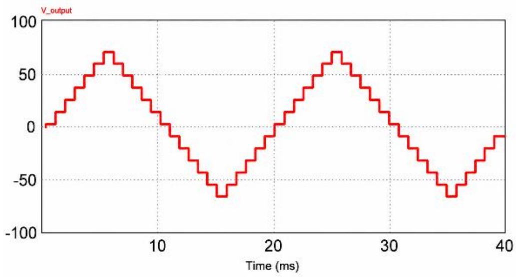

Figure 5. Voltage waveform for 13-level MLI in equal-step-angle switching

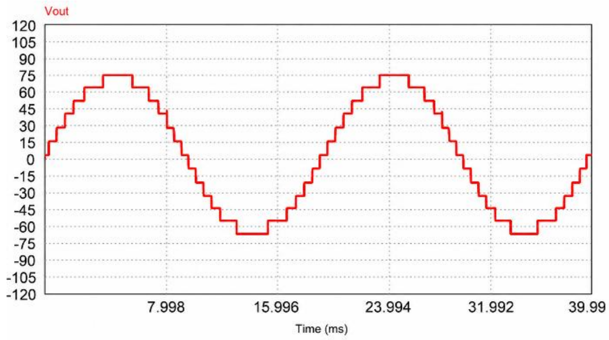

Figure 6. Voltage waveform for 13-level MLI in sinusoidal switching angle technique

In Figure 6, Vout on the y-axis denotes the output voltage (V), while the x-axis represents time in milliseconds (ms). The 13-level multilevel inverter (MLI) using the Sinusoidal Switching Angle Technique produces an output voltage waveform ranging from approximately −72 V to +72 V, comprising thirteen voltage levels that resemble a sinusoidal wave. The technique's effectiveness is demonstrated through adjusted switching angles that yield a symmetrical waveform, reduced total harmonic distortion (THD), lower switching stress, and improved output voltage quality.

Multilevel inverters are now widely used in industry for various applications [27]. Researchers and engineers worldwide continue to develop new topologies, control strategies, and operating techniques to improve their performance. These developments aim to enhance energy efficiency, reliability, and cost-effectiveness, making multilevel inverters increasingly attractive compared with conventional two-level topologies. In this system, the inverter is connected in series with an LC filter, which reduces high-order harmonics in the output voltage and provides a more sinusoidal voltage waveform to the load. As shown in Figure 7, the input voltage of the LC filter is determined by the switching state S(j) of the inverter and can be expressed as V_{in}= S(j)×$V_{dc,}$ where S(j) = 4-j, Vin is the input voltage of the LC filter, Vdc is the DC supply voltage, and S(j) is the switching function of the inverter, representing the switching state corresponding to each operating condition.

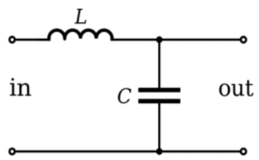

Figure 7. LC filter circuit

Two equations can be used to describe the LC filter, which is the depiction in the above Figure 7. The current through the filter inductance is represented by in (2).

$$L^{di}_{dt} = Vin - \mathrm{Vr} - \mathrm{Vc} \quad (2)$$

The capacitor voltage follows, which is represented in (3).

$$C^{di}_{dt} = iL - \mathrm{i0} \quad (3)$$

Where i is the total current flowing through the circuit. In case of this research, using this formula, we have calculated the values of the capacitor and inductor for a 13-level MLI. In both cases here used RC network capacitor value is C = 0.001 μF, and the value of inductance is L = 1 mH. The value of RC is determined using (4).

$$Fc = \frac{1}{2\pi\sqrt{(LC)}} \quad (4)$$

After applying the LC filter in 13-level MLI for both methods, the output voltage waveform is shown in Figure 8 and Figure 9.

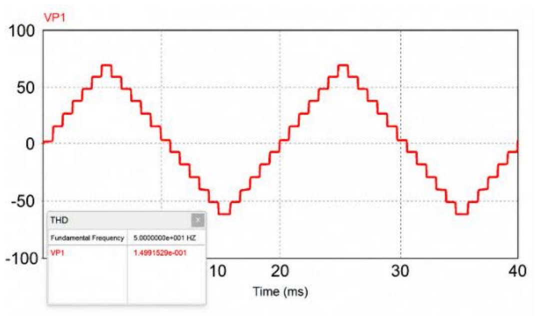

Figure 8. Voltage waveform for 13-level MLI in equal step angle technique after applying LC filter

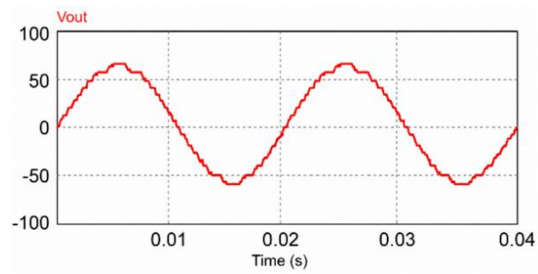

Figure 9. Output voltage waveform after applying lc filter in sinusoidal switching angle technique

The output waveform almost looks like a sine wave, which is the goal of this research: to convert DC to an AC signal. From the PSIM software, it will automatically generate the FFT signal & shows the THD value. The output waveform of the FFT signal with the THD value for the 13-level MLI is shown in Figure 10 and Figure 11.

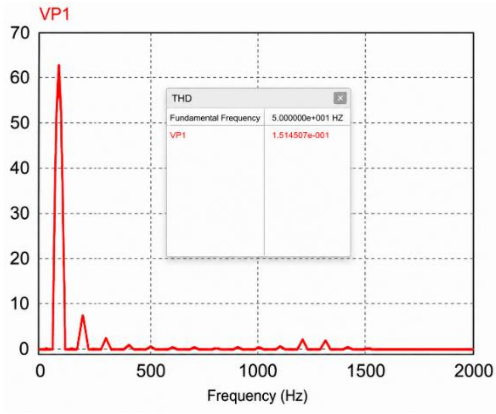

Figure 10. FFT and THD waveform after applying an LC filter in the equal-step switching angle technique

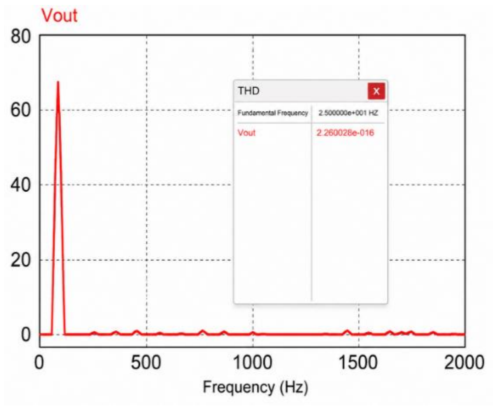

Figure 11. FFT and THD waveform after applying an LC filter in the sinusoidal switching angle technique

In both cases, Vout on the y-axis denotes the value of the output voltage, and the x-axis denotes the Fundamental Frequency. From Figure 9, it is obvious that after applying the LC filter, the output voltage waveform looks closer to an AC signal. The difference between the two techniques is shown in tabular form in Table 1. From Table 1, for the 13-level MLI, the lowest THD is found after applying the LC filter in a sinusoidal switching angle technique, and the highest is found when the filter is applied to the equal step angle switching. So, from this, it is proved that the sinusoidal technique reduces THD more as compared to other techniques.

Table 1. Different THD for two different techniques for 13-level MLI

Number of levels	For equal switching angle THD without LC filter	For equal switching angle THD with LC filter	For sinusoidal switching angle THD without LC filter	For sinusoidal switching angle THD with LC filter
13	17.44%	15.14%	7.12%	2.24%

Switching device stress analysis: As it is a 13-level asymmetrical MLI therefore IGBT voltage stress is different for different switches. Lower-level switches will experience lower stress, and higher-level switches will experience higher stress. To calculate the voltage stress instead of a single value, write in (5).

$$Vsw,k = Vdc,k \quad (5)$$

Where k = switching index and Vdc,k = DC source voltage. From this, Lower-level switches operate under lower voltage stress, while switches linked to the highest DC source endure the greatest voltage stress. Meanwhile, Current stress depends on the switching strategy, which is shown in (6).

$$I_{sw,rms}^{sin} > I_{sw,rms}^{EA} \quad (6)$$

Equal-angle switching improves current waveforms, leading to reduced RMS and peak current stress on IGBTs. A quantitative analysis of voltage and current is shown in Table 2.

It is observed that the sinusoidal switching angle achieves significantly lower THD compared to equal-angle switching under both filtered and unfiltered conditions. Without filtering, THD is reduced from 17.44% to 7.12%, and with LC filtering, it further decreases to 2.24%. Although equal-angle switching reduces switching frequency and associated losses, its harmonic performance in the present implementation is inferior due to non-optimized switching angles. The LC filter improves both cases; however, the improvement is more pronounced for the sinusoidal switching angle technique.

Table 2. Quantitative analysis table

Parameter	Sinusoidal switching angle	Equal switching angle	Improvement
Max voltage stress	36 V	36 V	0%
RMS current stress	2.10 pu	1.92 pu	↓ 9%
Peak current	Higher	Lower	Reduced
Switching frequency	High	Fundamental	Reduced losses
Switching loss	High	Low	Low
Conduction loss	Comparable	Comparable	Comparable
THD without LC filter	7.12%	17.44%	THD reduction in equal angle = ↓ 13.2%
THD with LC filter	2.24%	15.14%	THD reduction in sinusoidal switching angle = ↓ 68.5%

Switching loss and efficiency analysis: The total loss consists of conduction loss and switching loss, expressed as in (7).

$$P_{loss} = P_{cond} + P_{sw} \quad (7)$$

Where the conduction loss of each IGBT is calculated by (8):

$$P_{cond}, i = P_{CE(on)} \, . I_{avg}, i + R_{on}. \ I^2_{rms}, i \quad (8)$$

where $V_{CE(on)}$ represents the on-state voltage drop, R_{on} is the equivalent on-state resistance, and $I_{avg,i}$, $I_{rms,i}$ denote the average and RMS current through the i^{th} switch, respectively. Total conduction loss is shown in (9).

$$P_{\ cond} = \sum_{i=1}^{N} P_{\ cond} \ , i \quad (9)$$

The equation for the switching loss is shown in (10):

$$P_{\ sw} = fs \sum_{i=1}^{N} (E_{on} \ , i + E_{off}, i \quad (10)$$

where f_s is the switching frequency, and $E_{on,i}$, $E_{off,i}$ represent the turn-on and turn-off energy losses of the i^{th} device. From Table 2, sinusoidal switching exhibits better performance than equal-angle switching regarding THD, but it incurs higher switching losses due to its elevated switching frequency. Conversely, equal-angle switching reduces switching losses by functioning at fundamental frequency, leading to increased efficiency, albeit with higher harmonic distortion, as conduction losses remain similar for both methods.

For practical implementation, the researcher made a 13-level MLI. Figure 12. shows the resulting output waveform of the 13-level MLI using the proposed sinusoidal formula. After applying the LC filter, the practical output becomes more sinusoidal, although the zoomed-out view in Figure 13 reveals noticeable spikes in the waveform.

The proposed sinusoidal switching-angle method differs from conventional Equal-step angle and selective harmonic elimination. Unlike Equal-step angle, which requires solving linear equations to eliminate specific harmonics, the proposed method employs uniformly spaced switching angles within each quarter cycle. This eliminates the need for optimization algorithms or complex computations, resulting in a simpler control structure.

The sinusoidal output voltage waveform exhibits a spike due to the concurrent operation of switching devices, particularly when one IGBT turns off while another turns on. Research has indicated that implementing improved dead time control techniques can help mitigate these voltage spikes associated with switching. A comparison of the work is shown in Table 3.

Table 3. Level vs previous work vs their findings vs our findings

Level	Previous work	Their findings	Our findings	
		THD in equal switching angle technique	THD in equal switching angle technique	THD in sinusoidal switching angle technique
13	In reference [10], “A new multilevel inverter topology with reduced switch count”	15.12%	15.14%	2.24%

A 13-level inverter's THD performance is compared with published findings in Table 3. Using the equal switching angle methodology, the [10] obtained a THD of 15.12%, whereas the current study produces a similar THD of 15.14%. The suggested sinusoidal switching angle (SSA) method, on the other hand, significantly improves output voltage quality by lowering the THD to 2.24%.

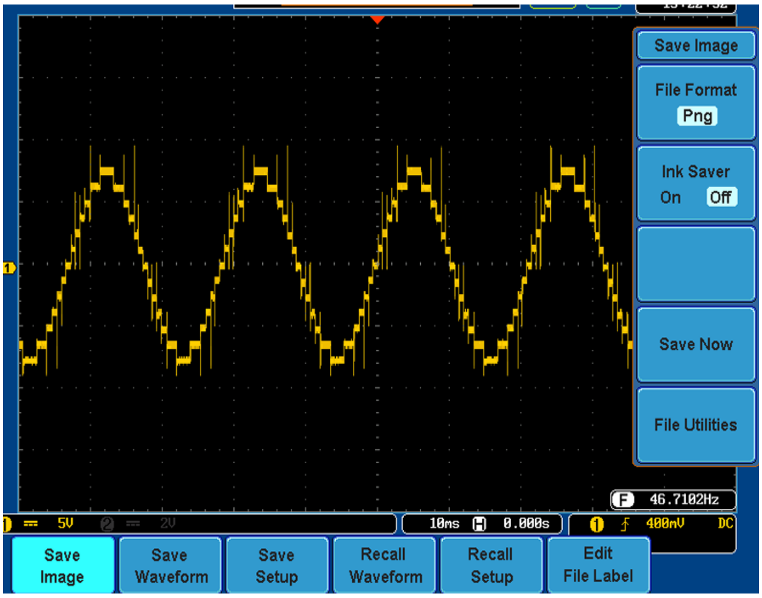

Figure 12. Practical output waveform for 13-level MLI

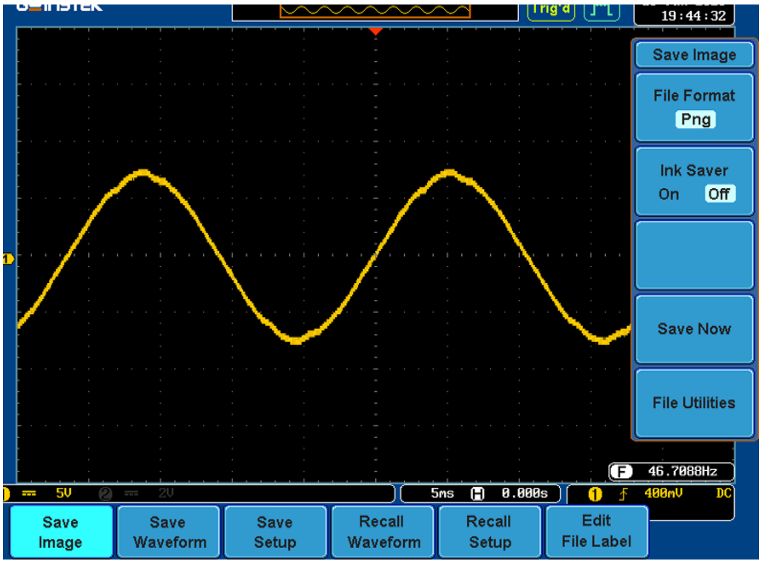

Figure 13. After applying the LC filter

4. CONCLUSION

The work compares equal-step and sinusoidal switching-angle control methods for a 13-level asymmetric cascaded H-bridge multilevel inverter. Testing showed that the sinusoidal angle method significantly reduced output voltage harmonic distortion, with THD decreasing from 15.14% to 2.24% after LC filtering. This indicates that sinusoidal switching angles improve waveform quality and provide an efficient means for harmonic reduction while maintaining a low switching frequency. Overall, the experimental and modeling results showed good agreement, although the hardware prototype displayed switching spikes due to non-ideal effects, contrasting the simulation's ideal assumptions. Enhanced techniques like dead-time optimization or snubber circuits may improve waveform quality in real applications. The proposed method uses a simple switching-angle calculation, offering a practical alternative to complex modulation techniques while achieving acceptable harmonic performance. The study focuses on waveform quality and THD reduction, leaving aspects like converter efficiency and long-term dependability for future research.

Future research will expand the suggested approach to higher-level multilevel inverter configurations, examine switching-loss and efficiency analysis, apply useful spike-mitigation techniques, contrast the suggested approach with sophisticated modulation strategies like selective harmonic elimination (SHE-PWM), and assess the strategy using real-time digital controllers in motor-drive and renewable energy applications. The effect of the suggested switching-angle technique on motor-drive performance, including torque ripple, speed stability, efficiency, and power losses in induction motor and BLDC drive applications, will be experimentally assessed in future work.

This study primarily focuses on the reduction of total harmonic distortion (THD) in a 13-level asymmetric cascaded H-bridge multilevel inverter using sinusoidal switching-angle control. The simulation was performed under ideal IGBT switching conditions, while the experimental validation was limited to a laboratory-scale prototype. Although the proposed method demonstrated significant THD reduction, comprehensive analyses of converter efficiency, switching and conduction losses, motor-drive performance, and long-term reliability were beyond the scope of this work. Furthermore, the proposed approach was validated only for the investigated inverter configuration; its scalability to higher-level multilevel inverters and real-time DSP/FPGA implementation requires further investigation.

ACKNOWLEDGMENTS

The study's partial financing was provided by the University of Asia Pacific's Institute for Research, Innovation and Development (IRID) in Dhaka, Bangladesh, which the authors acknowledge.

FUNDING INFORMATION

The authors state that no funding was involved for this research.

AUTHOR CONTRIBUTIONS STATEMENT

This journal uses the Contributor Roles Taxonomy (CRediT) to recognize individual author contributions, reduce authorship disputes, and facilitate collaboration.

Name of Author	C	M	So	Va	Fo	I	R	D	O	E	Vi	Su	P	Fu
Dewan Ashikur Rahaman	✓	✓	✓	✓	✓	✓	✓	✓	✓	✓	✓	✓	✓	✓
Aive Alamgir	✓	✓	✓			✓	✓	✓	✓	✓	✓	✓		
Md Ashraf Hossain		✓		✓		✓		✓		✓		✓		✓
Tapan Kumar Chakraborty	✓	✓		✓	✓		✓	✓	✓		✓	✓		
Raisul Islam Rafi	✓	✓		✓		✓	✓		✓	✓	✓	✓		
Raiyan Rahman Zihad	✓	✓	✓		✓			✓	✓	✓	✓		✓	✓
Md. Abdullah Al Mahmud	✓	✓		✓		✓	✓		✓	✓			✓	✓
Samia Sarkar	✓	✓	✓		✓	✓	✓	✓	✓	✓	✓	✓		

C : **C**onceptualization	I : **I**nvestigation	Vi : **Vi**sualization
M : **M**ethodology	R : **R**esources	Su : **Su**pervision
So : **So**ftware	D : **D**ata Curation	P : **P**roject administration
Va : **Va**lidation	O : Writing - **O**riginal Draft	Fu : **Fu**nding acquisition
Fo : **Fo**rmal analysis	E : Writing - Review & **E**diting	

CONFLICT OF INTEREST STATEMENT

Authors state no conflict of interest.

DATA AVAILABILITY

The data that support the findings of this study are available from the corresponding author, [DAR], upon reasonable request.

REFERENCES

[1] M. H. Rashid, *Power Electronics: Devices, Circuits, and Applications, International Edition*. Pearson, 2014.

[2] J. Rodriguez *et al.*, "Multilevel Converters: An enabling technology for high-power applications," *Proceedings of the IEEE*, vol. 97, no. 11, pp. 1786–1817, Nov. 2009, doi: 10.1109/JPROC.2009.2030235.

[3] D. A. Rahaman and T. K. Chakraborty, "Study of asymmetrical-multi level inverter using two switching angle techniques," *International Journal of Power Electronics and Drive Systems (IJPEDS)*, vol. 16, no. 4, p. 2570, Dec. 2025, doi: 10.11591/ijpeds.v16.i4.pp2570-2581.

[4] R. Barzegarkhoo, M. Forouzesh, S. S. Lee, F. Blaabjerg, and Y. P. Siwakoti, "Switched-capacitor multilevel inverters: a comprehensive review," *IEEE Transactions on Power Electronics*, vol. 37, no. 9, pp. 11209–11243, Sep. 2022, doi: 10.1109/TPEL.2022.3164508.

[5] N. Mukundan C M *et al.*, "A new multilevel inverter based grid connected reliable solar power transfer unit with power quality enhancement," *IEEE Transactions on Industry Applications*, vol. 59, no. 2, pp. 1887–1900, Mar. 2023, doi: 10.1109/TIA.2022.3218523.

[6] A. R. Lopez, C. J. Cortes, C. A. Limones-Pozos, J. M. Sosa, J. Aguayo, and S. De Leon Aldaco, "Optimal switching angles calculation for a multilevel inverter through the SHE method and the PSO algorithm, a comparison," in *2020 IEEE International Autumn Meeting on Power, Electronics and Computing (ROPEC)*, IEEE, Nov. 2020, pp. 1–6. doi: 10.1109/ROPEC50909.2020.9258680.

[7] C. I. Odeh, A. Lewicki, and M. Morawiec, "A single-carrier-based pulse-width modulation template for cascaded h-bridge multilevel inverters," *IEEE Access*, vol. 9, pp. 42182–42191, 2021, doi: 10.1109/ACCESS.2021.3065743.

[8] A. A. Theresa, K. Kalpana, and M. Nirmala, "A novel 31 level cascaded H-bridge inverter," in *2021 International Conference on Advance Computing and Innovative Technologies in Engineering (ICACITE)*, IEEE, Mar. 2021, pp. 228–233. doi: 10.1109/ICACITE51222.2021.9404703.

[9] K. K. Gupta, A. Ranjan, P. Bhatnagar, L. K. Sahu, and S. Jain, "Multilevel inverter topologies with reduced device count: a review," *IEEE Transactions on Power Electronics*, vol. 31, no. 1, pp. 135–151, Jan. 2016, doi: 10.1109/TPEL.2015.2405012.

[10] M. D. Siddique, S. Mekhilef, N. M. Shah, A. Sarwar, A. Iqbal, and M. A. Memon, "A new multilevel inverter topology with reduce switch count," *IEEE Access*, vol. 7, pp. 58584–58594, 2019, doi: 10.1109/ACCESS.2019.2914430.

[11] J. Rodriguez, Jih-Sheng Lai, and Fang Zheng Peng, "Multilevel inverters: a survey of topologies, controls, and applications," *IEEE Transactions on Industrial Electronics*, vol. 49, no. 4, pp. 724–738, Aug. 2002, doi: 10.1109/TIE.2002.801052.

[12] R. Shalchi Alishah, S. H. Hosseini, E. Babaei, and M. Sabahi, "Optimization assessment of a new extended multilevel converter topology," *IEEE Transactions on Industrial Electronics*, vol. 64, no. 6, pp. 4530–4538, Jun. 2017, doi: 10.1109/TIE.2017.2669885.

[13] M. A. Hosseinzadeh, M. Sarebanzadeh, C. F. Garcia, E. Babaei, and J. Rodriguez, "An asymmetric switched-capacitor multicell inverter with low number of DC source and voltage stress for renewable energy sources," *IEEE Access*, vol. 10, pp. 30513–30525, 2022, doi: 10.1109/ACCESS.2022.3140786.

[14] N. Prabaharan and K. Palanisamy, "A comprehensive review on reduced switch multilevel inverter topologies, modulation techniques and applications," *Renewable and Sustainable Energy Reviews*, vol. 76, pp. 1248–1282, Sep. 2017, doi: 10.1016/j.rser.2017.03.121.

[15] V. F. Pires, A. Cordeiro, D. Foito, J. F. Silva, and E. Romero-Cadaval, "Cascaded multilevel structure with three-phase and single-phase h-bridges for open-end winding induction motor drive," *IEEE Open Journal of the Industrial Electronics Society*, vol. 4, pp. 346–361, 2023, doi: 10.1109/OJIES.2023.3309652.

[16] J. P. R. A. Mello and C. B. Jacobina, "Single-phase converter with shared leg and generalizations," *IEEE Transactions on Power Electronics*, vol. 33, no. 6, pp. 4882–4893, Jun. 2018, doi: 10.1109/TPEL.2017.2734642.

[17] M. Aleenejad, H. Mahmoudi, R. Ahmadi, and H. Iman-Eini, "A new high-switching-frequency modulation technique to improve the DC-link voltage utilization in multilevel converters," *IEEE Transactions on Industrial Electronics*, vol. 64, no. 3, pp. 1807–1817, Mar. 2017, doi: 10.1109/TIE.2016.2623256.

[18] I. Khan and A. Mehrizi-Sani, "Switching angle prediction with artificial neural network for complete and partial selective harmonic elimination of multilevel inverters," in *2021 IEEE Power & Energy Society General Meeting (PESGM)*, IEEE, Jul. 2021, pp. 1–5. doi: 10.1109/PESGM46819.2021.9638105.

[19] B. Das, D. Chatterjee, and A. Bhattacharya, "Multilevel converter topology suitable for separate and variable magnitude of DC sources," *International Journal of Power Electronics*, vol. 15, no. 2, p. 194, 2022, doi: 10.1504/IJPELEC.2022.121409.

[20] E. Samadaei, S. A. Gholamian, A. Sheikholeslami, and J. Adabi, "An envelope type (E-Type) module: asymmetric multilevel inverters with reduced components," *IEEE Transactions on Industrial Electronics*, vol. 63, no. 11, pp. 7148–7156, Nov. 2016, doi: 10.1109/TIE.2016.2520913.

[21] E. Samadaei, A. Sheikholeslami, S. A. Gholamian, and J. Adabi, "A square t-type (ST-Type) module for asymmetrical multilevel inverters," *IEEE Transactions on Power Electronics*, vol. 33, no. 2, pp. 987–996, Feb. 2018, doi: 10.1109/TPEL.2017.2675381.

[22] E. Babaei, S. Alilu, and S. Laali, "A new general topology for cascaded multilevel inverters with reduced number of components based on developed H-bridge," *IEEE Transactions on Industrial Electronics*, vol. 61, no. 8, pp. 3932–3939, Aug. 2014, doi: 10.1109/TIE.2013.2286561.

[23] Y. Wang, K. Wang, and G. Li, "A generalized switched-capacitor step-up multilevel inverter employing single DC source," *CSEE Journal of Power and Energy Systems*, vol. 8, no. 2, pp. 439–451, 2021, doi: 10.17775/CSEEJPES.2020.06280.

[24] K. Panda, P. Bana, O. Kiselychnyk, J. Wang, and G. Panda, "A single-source switched-capacitor-based step-up multilevel inverter with reduced components," *IEEE Transactions on Industry Applications*, vol. 57, no. 4, pp. 3801–3811, Jul. 2021, doi: 10.1109/TIA.2021.3068076.

[25] M. N. Hamidi, D. Ishak, M. A. A. M. Zainuri, and C. A. Ooi, "Multilevel inverter with improved basic unit structure for symmetric and asymmetric source configuration," *IET Power Electronics*, vol. 13, no. 7, pp. 1445–1455, May 2020, doi: 10.1049/iet-pel.2019.0916.
[26] E. Robles, M. Fernandez, J. Zaragoza, I. Aretxabaleta, I. M. De Alegria, and J. Andreu, "Common-mode voltage elimination in multilevel power inverter-based motor drive applications," *IEEE Access*, vol. 10, pp. 2117–2139, 2022, doi: 10.1109/ACCESS.2021.3137892.
[27] M. Trabelsi, H. Vahedi, and H. Abu-Rub, "Review on single-DC-source multilevel inverters: topologies, challenges, industrial applications, and recommendations," *IEEE Open Journal of the Industrial Electronics Society*, vol. 2, pp. 112–127, 2021, doi: 10.1109/OJIES.2021.3054666.

BIOGRAPHIES OF AUTHORS

Dewan Ashikur Rahaman is a lecturer in the Department of Electrical and Electronic Engineering at the University of Asia Pacific (UAP), Dhaka, Bangladesh. He received his B.Sc. in Electrical and Electronic Engineering from the University of Asia Pacific in 2022. He has been serving as a lecturer at UAP since 2024. His research interests include power system analysis, power system contingency analysis, power system stability, power electronics, renewable energy, embedded systems, artificial intelligence, intelligent control, and digital libraries. He can be contacted at email: ashik@uap-bd.edu.

Aive Alamgir received her B.Sc. in electrical and electronic engineering from the University of Asia Pacific in 2023. Her research interests include power system analysis, power system contingency analysis, power system stability, power electronics, and renewable energy. She can be contacted at email: aivealamgir50@gmail.com.

Md Ashraf Hossain received his B.Sc. in electrical and electronic engineering from the University of Asia Pacific in 2022. His research interests include power system analysis, power system stability, power electronics, and renewable energy. He can be contacted at email: ashrafhossain2023@outlook.com.

Dr. Tapan Kumar Chakraborty received his Bachelor of Science degree in electrical and electronic engineering from the Bangladesh University of Engineering and Technology (BUET), Dhaka, in 1984. He completed his M.Eng. degree in electrical engineering at the University of Roorkee, India, in 1988, and obtained his Ph.D. degree in electrical and computer engineering from Kanazawa University, Japan, in 1998. He served as a lecturer, assistant professor, associate professor, and professor in the Department of Electrical and Electronic Engineering at Dhaka University of Engineering and Technology (DUET) from October 1988 to May 2005. From May 2005 to September 2016, he served as a professor and chairman of the Department of Electrical and Computer Engineering at Presidency University, Dhaka. In September 2016, he joined the Department of Electrical and Electronic Engineering at the University of Asia Pacific, Dhaka, as a professor. He has authored more than forty research papers published in journals and presented at national and international conferences. His research interests include electronic materials and devices, phase-change memory, electronic circuits, and power electronics. He is a fellow of the Institution of Engineers, Bangladesh (IEB), and a member of the IEEE. He can be contacted at email: tkc@uap-bd.edu.

Raisul Islam Rafi is a regular B.Sc. student in the Department of Electrical and Electronic Engineering at the University of Asia Pacific (UAP), Dhaka, Bangladesh. His research interests include power system stability, high-voltage direct current (HVDC) systems, and flexible AC transmission systems (FACTS). He can be contacted at email: 23108031@uap-bd.edu.

Raiyan Rahman Zihad is a regular B.Sc. student in the Department of Electrical and Electronic Engineering at the University of Asia Pacific (UAP), Dhaka, Bangladesh. His research interests include power system stability, high-voltage direct current (HVDC) systems, and flexible AC transmission systems (FACTS). He can be contacted at email: 23108039@uap-bd.edu.

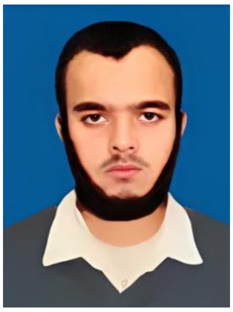

Md. Abdullah Al Mahmud is an assistant professor in the Department of Electrical and Electronic Engineering at the University of Asia Pacific (UAP), Dhaka, Bangladesh. He received his B.Sc. degree in electrical and electronic engineering from the University of Asia Pacific in 2013. His research interests include biomedical engineering and signal processing. He can be contacted at email: abdullah-eee@uap-bd.edu.

Samia Sarkar is a regular B.Sc. student in the Department of Electrical and Electronic Engineering at the University of Asia Pacific (UAP), Dhaka, Bangladesh. Her research interests include power system stability, high-voltage direct current (HVDC) systems, and flexible AC transmission systems (FACTS). She can be contacted at email: 23108023@uap-bd.edu